Journal of ELECTRONIC MATERIALS, Vol. 47, No. 10, 2018
https://doi.org/10.1007/s11664-018-6565-2

Investigation of MBE-Growth of Mid-Wave Infrared $Hg_{1-x}Cd_xSe$

I. MADNI,[1,2] G.A.U. MEMBRENO,[1] W. LEI,[1] and L. FARAONE[1]

1.—School of Electrical, Electronic and Computer Engineering, The University of Western Australia, Crawley, WA 6009, Australia. 2.—e-mail: imtiaz.madni@gmail.com

Undoped mid-wave infrared $Hg_{1-x}Cd_xSe$ epitaxial layers have been grown to a nominal thickness of 8–14 μm on GaSb (211)B substrates by molecular beam epitaxy (MBE) using constant beam equivalent pressure ratios. The effects of growth temperature from 70°C to 120°C on epilayer quality and its electronic parameters has been examined using x-ray diffraction (XRD) rocking curves, atomic force microscopy, Nomarski optical imaging, photoconductive decay measurements, and variable magnetic field Hall effect analysis. For samples grown at 70°C, the measured values of XRD rocking curve full width at half maximum (FWHM) (116 arcsec), root mean square (RMS) surface roughness (2.7 nm), electron mobility (6.6×10^4 cm^2 V^{-1} s^{-1} at 130 K), minority carrier lifetime ($\sim$ 2 μs at 130 K), and background n-type doping ($\sim 3 \times 10^{16}$ cm^{-3} at 130 K), indicate device-grade material quality that is significantly superior to that previously published in the open literature. All of these parameters were found to degrade monotonically with increasing growth temperature, although a reasonably wide growth window exists from 70°C to 90°C, within which good quality HgCdSe can be grown via MBE.

Key words: HgCdSe, MBE, alternatives to HgCdTe, II–VI materials, infrared detectors

INTRODUCTION

Over the past several decades, the material of choice for high-performance infrared detection has been mercury cadmium telluride (HgCdTe),[1,2] primarily because of its unsurpassed optoelectronic properties and because its bandgap can be tuned to absorb light with wavelengths from short wave infrared (SWIR) to very long wave infrared (VLWIR).[3] High quality semiconducting HgCdTe with reasonably low dislocation densities $\sim 10^5$ cm^{-2} can be grown by molecular beam epitaxy (MBE) on lattice-matched cadmium zinc telluride (CdZnTe) substrates.[1] However, the use of CdZnTe for large area focal plane arrays is limited by the maximum size of commercially available CdZnTe available, which is around 50 cm^2. Alternative large-area substrates, such as GaAs,[4,5] Ge,[6] Si,[7] and GaSb,[8–10] have been proposed for the growth of HgCdTe by MBE. Although these alternative substrates are available in sizes as large as 6 in. in diameter, they have a large lattice mismatch with HgCdTe: 14%, 17%, and 6% for GaAs, Si, and GaSb, respectively, which results in high dislocation densities that degrade device performance, particularly for LWIR HgCdTe.[11]

Semiconducting mercury cadmium selenide (HgCdSe) has been proposed as an alternative Hg-based material for infrared detection since, similar to the HgCdTe ternary alloy, the bandgap of HgCdSe can be engineered to detect wavelengths ranging from SWIR to VLWIR.[12] In addition, HgCdSe belongs to the family of semiconductors with lattice parameters around 6.1 Å, which includes many lattice-matched and nearly lattice-matched substrates that are available in large sizes ranging from 4 in. to 6 in. in diameter, including GaSb.[8] Several materials with bandgaps suitable for detection of light in the visible and ultraviolet spectral ranges also belong to the 6.1 Å family, raising the possibility of creating multi-layer heterostructure devices using various nearly

(Received January 27, 2018; accepted July 31, 2018; published online August 9, 2018)

lattice-matched materials that can detect wavelengths from ultraviolet to the VLWIR.

It is surprising to note that, whereas MBE growth of thin HgCdTe-based structures have been studied extensively, there has been very little work reported in the open literature on MBE-grown HgCdSe epilayers or related materials. Lansari et al.[13] reported the first epitaxial growth of HgSe and $Hg_{1-x}Cd_xSe$ thin films by MBE, and studied their optical, electrical, and structural properties. The substrates used in their study included both (100) and (211)B oriented CdZnTe and ZnTe single crystals, and the growth temperatures investigated in their experiments were between 80°C and 150°C. They varied the beam equivalent pressures (BEPs) of mercury and selenium in the range from 5.33×10^{-6} kPa to 2×10^{-5} kPa and from 8×10^{-8} kPa to 1.33×10^{-7} kPa, respectively. Results of the MBE growth of HgCdSe on Si substrates has been presented by Doyle et al.,[14] which included a study of the effect of different Se source materials on the electron concentration in as-grown HgCdSe.

In this work, we demonstrate the MBE growth of mid-wave infrared (MWIR) HgCdSe on GaSb(211)B substrates. GaSb is closely lattice-matched with HgCdSe, and epi-ready large-area substrates are readily available from multiple commercial suppliers. The HgCdSe samples were grown at different temperatures using the same Cd to Se and Hg to Se beam equivalent pressure (BEP) ratios. The effects of growth temperature on MBE-grown $Hg_{1-x}Cd_xSe$ epitaxial quality, and the associated variation in surface morphology and semiconducting properties, have been studied in this work. It is concluded that the optimal temperature range for MBE growth of HgCdSe is between 70°C and 90°C, and that the epilayers grown at higher temperature generally have poorer quality, as determined from x-ray diffraction (XRD) rocking curves and Nomarski optical microscopy studies of surface morphology, and from electronic transport and minority carrier lifetime measurements.

EXPERIMENTAL PROCEDURES

In this study, epi-ready GaSb (211)B substrates were used for MBE growth, which are closely lattice-matched to HgCdSe. Growth of MWIR HgCdSe epilayers was carried out in a mercury-compatible ultrahigh vacuum MBE system (Riber 32P), which is equipped with a barometer-type, externally reloadable, and temperature controlled mercury source, and selenium and cadmium containing effusion cells. Preliminary experiments were performed to optimize the MBE-growth conditions for HgCdSe thin films, which were based on systematic variation of film growth parameters such as Hg/Se flux ratio, growth temperature, mercury flux, and selenium flux. Hg (7 N), Cd (6 N), Se (5N5), Zn (6 N) and Te (6 N) were used as the source materials, and standard effusion cells were used to evaporate the source materials without cracking. GaSb substrates were treated thermally at 580°C to desorb the native oxides at surfaces. Thermal desorption was done in absence of background Sb flux in order to avoid cross-contamination in MBE growth chamber by Sb, which is often used as a p-type dopant for II-VI materials. After thermal cleaning, substrate temperatures were reduced to 320°C to grow thin buffer layers of ZnTe ($\sim$ 300 nm thick). HgCdSe epilayers were grown subsequently on ZnTe buffer layers at various growth temperatures (70–120°C). After the growth of HgCdSe, the samples were cooled to room temperature without any background Hg flux. A large Hg BEP ($\sim 10^{-5}$ kPa) was used to overcome deficiency of Hg due to its low sticking coefficient, while relatively lower BEP were used for Se ($\sim 10^{-7}$ kPa) and Cd ($\sim 10^{-8}$ kPa). *In situ* growth temperature was measured and monitored by thermocouple in contact with the molybdenum (Mo) block holding the substrates.

The growth temperature range investigated in the current study was between 70°C and 120°C, and the mercury and selenium beam equivalent pressures (BEPs) were kept constant for this study. The compositions for prominent infrared (IR) applications are obtained within the bulk-growth cubic phase range. Thus, for this reason, HgCdSe epilayers with composition restricted to $x \leq 0.3$ were grown in the present study to a nominal thickness between 8 μm and 14 μm. The structural properties of these MBE-grown layers were evaluated by means of Nomarski optical microscopy, atomic force microscopy (AFM), and double-crystal XRD. Reflectance/transmission measurements were undertaken using Fourier transform infrared (FTIR) spectroscopy to assess the optical properties of the epilayers. Electronic carrier transport parameters were measured by means of Van der Pauw variable magnetic field Hall effect measurements, and the minority carrier lifetime was extracted from photoconductive decay measurements. High resolution mobility spectrum analysis (HR-MSA) was performed on the Hall effect data, in order to distinguish the carrier transport parameters of the HgCdSe epilayers from contributions arising from carriers in the GaSb substrates, and to identify any multiple carrier species that may be present in the epilayers.

RESULTS AND DISCUSSION

The absorption cut-off wavelength was determined via FTIR transmittance measurements, and Fig. 1 shows the room-temperature transmittance profiles of individual samples grown at various substrate temperatures. The molar fraction of CdSe in the $Hg_{1-x}Cd_xSe$ alloy (x-value) was determined from these measurements using the relationship between bandgap and x-value developed by Summers and Broerman.[15] It was observed that the x-

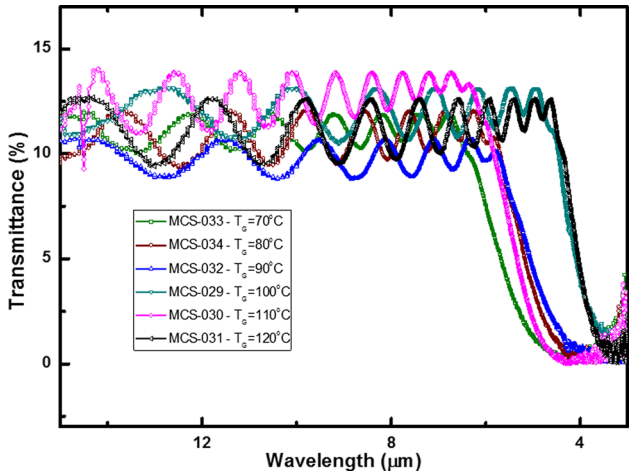

Fig. 1. Room-temperature FTIR transmission spectra of HgCdSe epilayers grown at various growth temperatures from 70°C to 120°C, and with a nominal thicknesses of 8–14 μm.

value for $Hg_{1-x}Cd_xSe$ suitable for detection in the mid-wave infrared (MWIR) region is ~ 0.2, whereas in the case of $Hg_{1-x}Cd_xTe$ it is ~ 0.3. A summary of main parameters obtained from characterization of samples used in this work can be seen in Table I. As shown in Fig. 1, transmittance percentages of all samples are relatively lower ($\sim 15\%$), which is due to highly conductive III–V substrate GaSb. High absorption and/or scattering from the n-doped GaSb substrate reduces the transmittance percentage. For high quality device fabrication, these substrates will need to be removed by etching.

The epilayer surface morphology was found to be strongly dependent on the growth temperature, and Fig. 2a, b, c, d, e and f shows surface images of the $Hg_{1-x}Cd_xSe$ epilayers grown at different temperatures, as observed by Nomarski optical microscopy. The characterization of surface morphology and related surface defects of MBE-grown materials is important, since they are a reflection of crystal growth mechanisms prevalent during MBE growth. It is evident from Fig. 2 that the optimum growth temperature exists within the lower temperature range, since increasing the growth temperature results in surface hillock formation and increasing surface roughness. As indicated in Fig. 2a, a mirror-like surface was observed for epilayers grown at 70°C, whereas for increasing growth temperatures the surface morphology gradually deteriorated even though the II/VI flux ratio was kept constant.

The surface peak-to-valley height of the sample grown at 120°C is in the range of 5–7 nm for a nominally 12 μm thick epilayer. The hillocks and/or needle-like defects apparent on the surfaces of samples grown at temperatures > 80°C have regular patterns, which are visible in Fig. 2c, d, e and f. The alignment of these surface defects is in the [213] direction, which is the line of intersection between a (211) surface plane and a (111) slip plane.

Table I. List of structural and electronic parameters for nominally 8–14 μm thick HgCdSe epilayers that were MBE grown at various temperatures in the course of this study, and comparison with previous values published in the open literature

Sample label	Substrate used	Growth temp. (°C)	Thickness (μm)	Cut-off wavelength at T = 298 K (μm)	X-value	FWHM rocking curve (arcsec)	RMS surface roughness (nm)	Electron conc. at 130 K (cm^{-3})	Electron mobility at 130 K (cm^2 V^{-1} s^{-1})	Minority carrier lifetime at 77 K (μs)
MCS-033	GaSb	70	14.1	5.46	0.19	116	2.7	3.1×10^{16}	~ 66000	~ 2
MCS-034	GaSb	80	12.8	4.07	0.22	151	3.01	3.5×10^{16}	~ 33000	~ 1.6
MCS-032	GaSb	90	7.9	4.16	0.22	202	3.14	3.5×10^{16}	~ 27000	~ 1.25
MCS-029	GaSb	100	12	5.7	0.18	216	3.95	7×10^{16}	~ 23000	~ 1.18
MCS-030	GaSb	110	11.7	5.2	0.19	223	4.7	5.8×10^{16}	~ 26500	~ 0.86
MCS-031	GaSb	120	8.8	5	0.20	234	5.43	1.18×10^{17}	~ 16000	~ 0.70
Doyle et al.[14]	Si	100	4–8	4–5	0.20	–	–	2×10^{17}–1×10^{18} @80 K	4000–15000 @80 K	–
Lansari et al.[13]	CdZnTe	100	2–3	3–6	0.11–0.34	350–400	–	$2–4 \times 10^{17}$ @80 K	2000–10000 @80 K	–
Brill et al.[22]	Si, GaSb	85–100	4–5	4–5	0.2	220–280	–	10^{17}–10^{18} @80 K	–	–

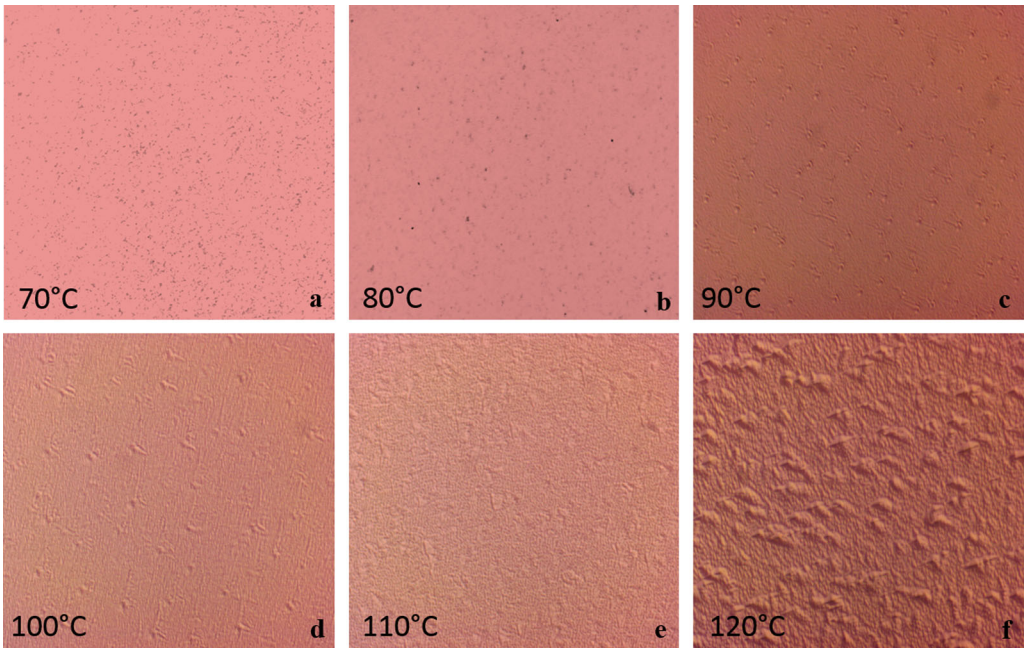

Fig. 2. Nomarski optical surface images of a 14 × 12 μm^2 area of nominally 8–14 μm thick HgCdSe epilayers grown at temperatures (a) 70°C, (b) 80°C, (c) 90°C, (d) 100°C, (e) 110°C, and (f) 120°C.

These surface features could be associated with slippage along these planes and, consequently, with dislocation and defect formation.[16] The isotropic stress associated with lattice vacancies, which would result from a reduction in net condensation flux at the higher growth temperatures, produces slip in the HgCdSe alloy along the existing symmetric (110) orientation and {111}-direction slip mechanisms to form dislocations. The net condensation flux at the growth surface depends upon the difference between the impinging flux from the sources and the re-evaporation flux from the surface. This flux difference multiplied by the condensation coefficient gives the actual condensation flux, which is predominantly determined by the growth temperature.[17] That is, at higher growth temperatures this mechanism results in a larger number of vacancies, a higher dislocation density and, consequently, a higher degree of surface roughness in MBE-grown HgCdSe.

Figure 3a shows XRD rocking curves of $Hg_{1-x}Cd_xSe$ epilayers grown under the same flux ratio, but at different temperatures, which indicates that the epilayer crystal quality is degraded with increasing growth temperature. Figure 3b illustrates the XRD rocking curve curve full width at half maximum (FWHM) of $Hg_{1-x}Cd_xSe$ epilayers as a function of growth temperature. From these measurements, it would appear that alloy disordering is less severe in $Hg_{1-x}Cd_xSe$ grown at the lower temperatures, with epilayers grown at 70°C having the smallest XRD rocking curve FWHM. The monotonically increasing value of rocking curve FWHM of epilayers grown at increasing growth temperature, is indicative of defect density in the crystal structure, which is also well-correlated with the observed decrease in the corresponding rocking curve relative peak intensity. In general, we observed an approximate doubling of XRD FWHM from 116 to 234 arcseconds as the $Hg_{1-x}Cd_xSe$ MBE growth temperature was increased from 70°C to 120°C.

Similar to HgCdTe, threading dislocations in a HgCdSe single crystal either move towards the surface and terminate, or form dislocation loops within the material. Given the large aspect ratio of the samples, and considering that generally MBE-grown single crystals have dislocation densities in the range from 10^4 cm^{-2} to 10^5 cm^{-2}, it becomes energetically more favorable to create dislocation loops at higher growth temperatures.[18,19] Therefore, threading dislocations can exhibit screw, edge, or mixed characteristics along the dislocation line depending on the angle between the Burgers vector and the dislocation line. Most of the observed surface features on the MBE-grown HgCdSe (211) samples in this study were very low in height, approximately 0.5 nm, which is slightly larger than one atomic step on a (211) surface. These surface features have well-aligned surface morphologies that are caused by surface strain relief, and are dominated by slight lattice deformation in samples grown at higher temperatures. Two competing mechanisms, surface strain relief and dislocation formation, can coexist within the same material, and the dominance of one over the other in HgCdSe epilayers is determined by the growth conditions and the thermal history of the sample, thus affecting the crystal quality for different growth temperatures.[19] The degradation of

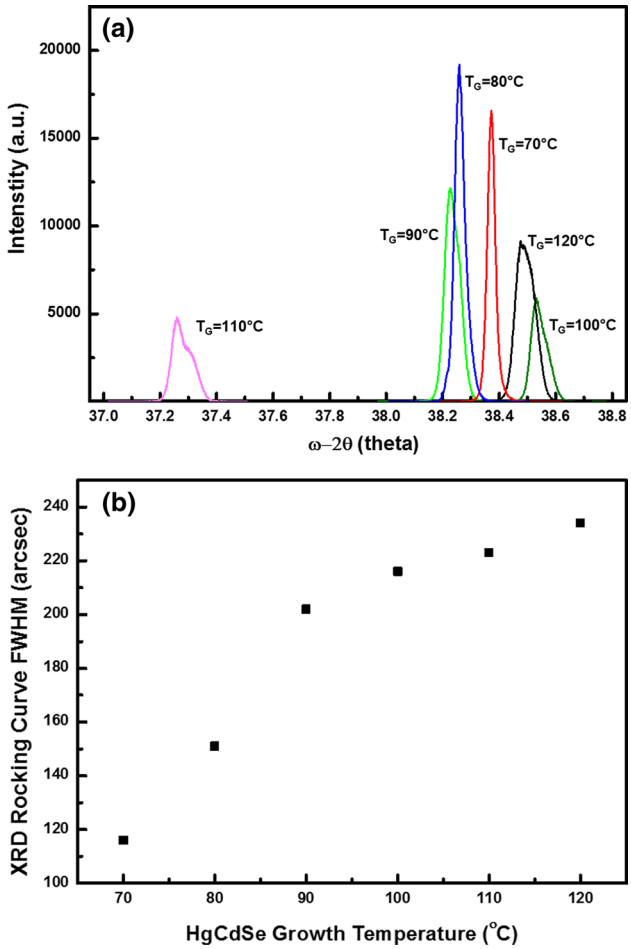

Fig. 3. (a) XRD rocking curves for HgCdSe epilayers grown at various growth temperatures (T_G), and (b) FWHM of XRD rocking curves of HgCdSe epilayers as a function of growth temperature.

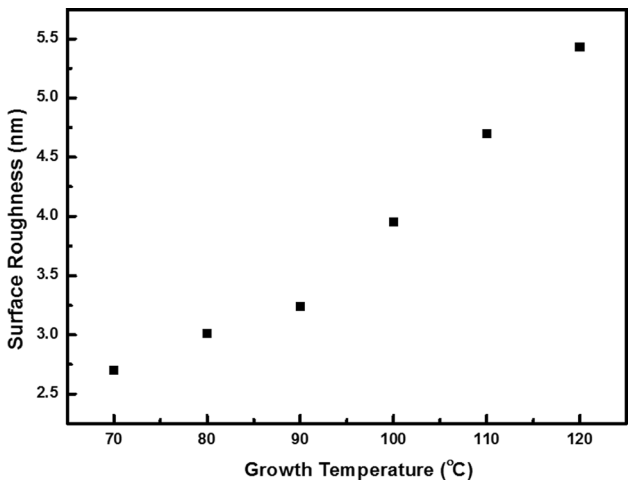

Fig. 4. RMS surface roughness, as determined by AFM measurements, of HgCdSe epilayers as a function of growth temperature.

HgCdSe crystal quality at high growth temperatures, as determined by XRD rocking curves, is well-correlated with that obtained from the analysis of surface morphology and surface roughness, as evident from Figs. 3 and 4.

The surface morphologies and surface height profiles of HgCdSe epilayers as a function of growth temperature, as measured by AFM, are shown in Fig. 5, which indicates that surface roughness increases rapidly at high growth temperatures. The lowest root mean square (RMS) surface roughness of $\sim$ 2.7 nm was obtained from samples grown at the lowest temperature used in this study, i.e. 70°C, and increased gradually with increasing growth temperature followed by a more rapid increase for samples grown above 90°C. Once again, these results are in good agreement with those obtained from the analysis of Nomarski optical images, and x-ray rocking curve measurements. The growth temperature induced variation in surface roughness and crystal quality could be due to the increased growth rate at higher temperatures, which may result in re-evaporation of atoms from the growing epilayers and forming vacancies and dislocations which, ultimately, will degrade the crystalline and surface quality.

The electronic transport properties (carrier concentration and mobility) of as-grown samples were determined using Van der Pauw Hall effect measurements with a standard 2T variable-field electromagnet system. Ohmic contacts were formed on the sample corners using pressed indium bumps after scouring the sample corners to ensure a good connection to both the epilayer and substrate. High resolution mobility spectrum analysis (HR-MSA) was applied to the raw data obtained from the variable magnetic field Hall measurements, which allows identification of multiple carrier species in the epilayers, and allows conduction contributions from the substrate and epilayer to be separated.[20] Figure 6a shows the low temperature electron mobility spectrum for the GaSb substrate, where it is evident that the substrate contains two n-type carrier species. A representative mobility spectrum for the epilayers is shown in Fig. 6b, which illustrates the analysis for sample MCS-033, grown at 70°C. HR-MSA is capable of extracting net carrier concentration and mobility for each of the species contributing to the transport. Clearly, the magnitude of the contribution of the GaSb substrate to conductivity in samples with HgCdSe epilayers is not of the same order as measured in the GaSb substrate alone. In order to remove any ambiguity, the samples were measured and analyzed repeatedly, and with different measurement configurations, which resulted in approximately the same outcome. The reduced contribution of the substrate to the total sample conductivity shown in Fig. 6b is likely to be due to the presence of the wide bandgap ZnTe buffer layer between the substrate and epilayer. Two distinct electron carrier species with clearly defined mobility were observed in all $Hg_{1-x}Cd_xSe$ epilayers grown in this study, and the analysis indicated that there was no contribution to

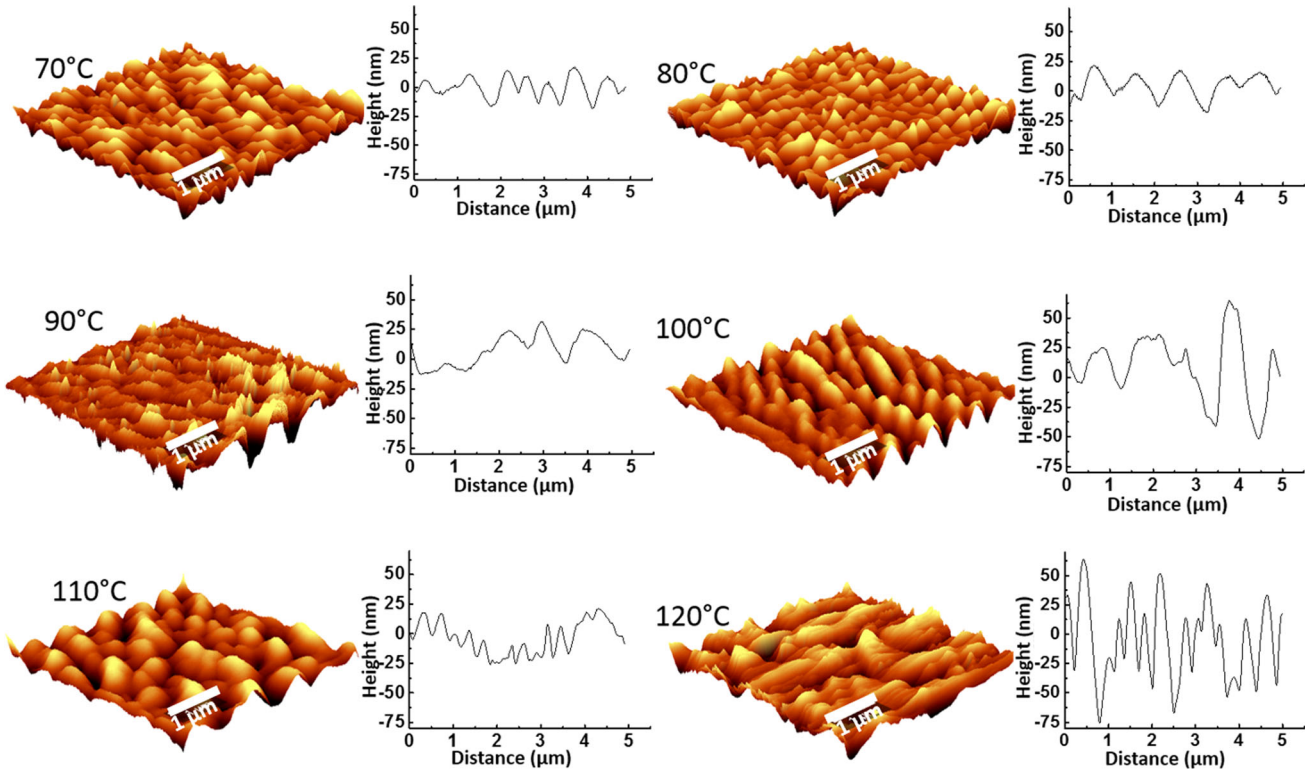

Fig. 5. AFM images and surface height profiles of an area of 5 × 5 μm^2 of HgCdSe epilayers grown at various temperatures.

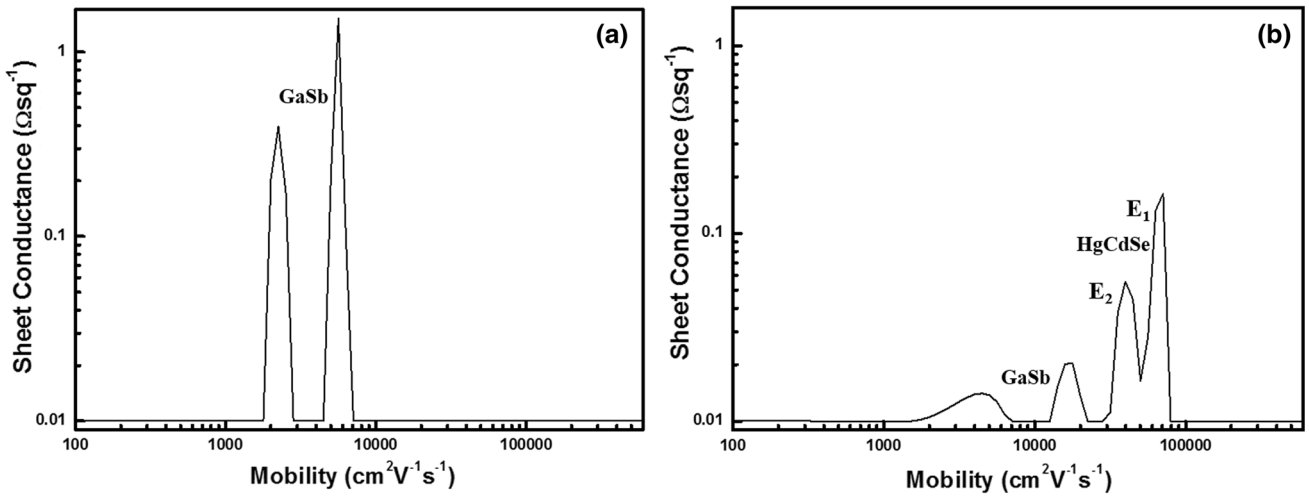

Fig. 6. Electron mobility spectra measured at 130 K in (a) GaSb substrate only, and (b) $Hg_{1-x}Cd_xSe$-on-GaSb epilayer grown at 70°C (MCS-033).

the conductivity from any hole species. The free electrons in these intentionally undoped samples are usually attributed to Se vacancies, which render as-grown HgCdSe epilayers n-type, although impurities from the MBE source materials cannot be ruled given that 7 N purity Se is not readily available. It is likely that the low mobility carrier in the epilayer (labelled as E2 in Fig. 6b), is contributed by a surface accumulation layer, since the Hall measurements were undertaken without surface treatment or passivation. The concentration of the dominant E1 electron species remained high as the MBE-growth temperature was increased from 70°C to 120°C and, as shown in Fig. 7, the concentration increased monotonically with increasing growth temperature. The observed n-type carrier concentration is relatively constant and in the low 10^{16} cm^{-3} range for an MBE-growth temperature up to 90°C, which is significantly lower than any previous values reported in the open literature

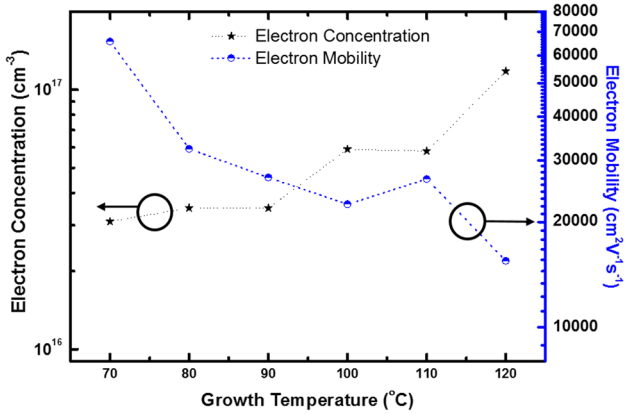

Fig. 7. Electron carrier concentration and mobility of electrons (high mobility E_1 carrier only) measured at 130 K in HgCdSe epilayers as a function of MBE-growth temperature.

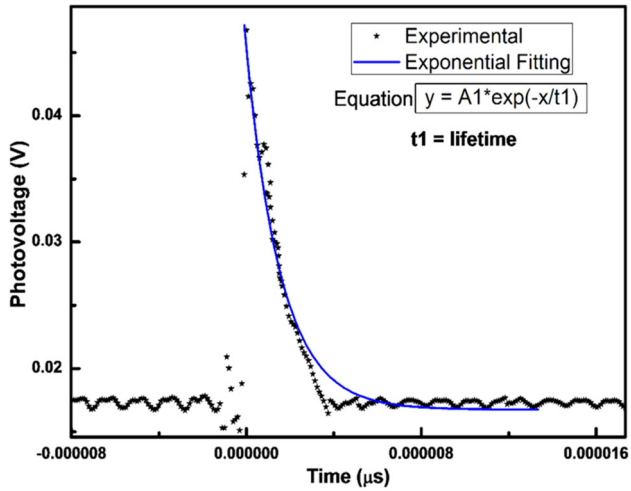

Fig. 8. Representative curve for photoconductive decay measurement of HgCdSe sample grown at 70°C. Inset shows the equation used for exponential fitting of photoconductive decay curve to extract minority carrier lifetime.

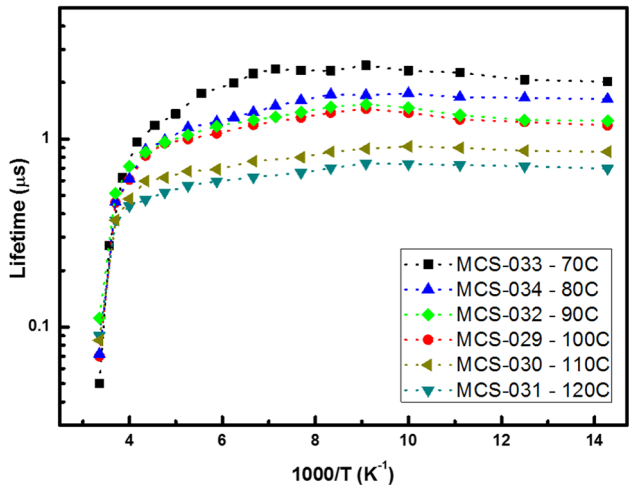

Fig. 9. Experimental minority carrier lifetime as a function of temperature for HgCdSe epilayers grown at various temperatures.

for undoped HgCdSe, which were in the range of 10^{17}–10^{18} cm^{-3}.[13]

The electron mobility for the dominant E_1 carrier was extracted from Hall effect measurements at 130 K for all samples, and the values are shown in Fig. 7, which indicates a significant decrease in electron mobility with increasing sample growth temperature. This observed trend is qualitatively consistent with an increase of crystalline-disorder scattering due to degradation of the crystal quality at higher growth temperatures, as noted previously from analysis of XRD and surface morphology results. It is noted that the electron mobility of these samples at 130 K ranged from 1.5×10^4 cm^2 V^{-1} s^{-1} to 6.6×10^4 cm^2 V^{-1} s^{-1} for MBE growth temperatures of 120°C and 70°C, respectively, which is considerably higher than any previously reported values by other workers.[13,14]

Photoconductive decay experiments were undertaken to evaluate the minority carrier lifetime in the samples grown at different temperatures. The representative original curve of photoconductive decay in sample grown at 70°C is shown in Fig. 8. Minority carrier lifetimes extracted from exponential fitting of photoconductive decay measurements as a function of measurement temperature are shown in Fig. 9, and indicate a clear correlation between minority carrier lifetime and growth temperature. The observed trend is similar to all other measurements and analysis undertaken in this study: that is, the sample grown at 70°C had the longest minority carrier lifetime, and the lifetime was found to decrease with increasing growth temperature for the other samples. A considerably long lifetime of ~ 2.1 μs was measured at 70 K for the sample grown at 70°C. For narrow bandgap semiconductors such as HgCdSe, band-to-band Auger-1 recombination usually controls the minority carrier lifetime, where electron–electron collisions and hole–hole collisions result in energy loss and subsequent Auger-1 recombination. However, in an extrinsic semiconductor the temperature dependence of the Auger-1 lifetime is not as strong as in an intrinsic semiconductor. As shown in Fig. 9, Auger-1 recombinations can be identified by analyzing the lifetime measurements as a function of temperature, due to the strong temperature dependence of the Auger-1 lifetime. Therefore, the increase in electron concentrations, and degradation of the crystal quality with increasing growth temperature, is the reason for the shorter lifetime observed in samples grown at higher temperatures. However, despite the high electron concentration, the minority carrier lifetime for all these samples is relatively long, which indicates a high quality material growth and a low concentration of SRH centers.

Table I lists the important parameters for each sample grown via MBE at various growth temperatures as part of this study, as well as

representative values for HgCdSe materials grown by other workers.[13,14] Our results indicate that the growth of good quality HgCdSe epilayers can be achieved within a growth window of at least 70–90°C, which is much wider than the typical 5°C growth window for HgCdTe epilayers. This improvement can be better understood by considering the fact that the formation of HgCdSe epilayers is the result of various competing growth mechanisms between binary compounds HgSe and CdSe, similar to that whereby HgCdTe epilayers are formed as an alloy of the CdTe and HgTe binary compounds. Since the bond length of CdSe is shorter than that of CdTe, it would be expected that the binding energy of the CdSe binary compound is greater than that of CdTe. In addition, the heats of atomization and formation for CdSe are 57 $kcal^{-1}$ g $atom^{-1}$ and 32.5 $kcal^{-1}$ g $atom^{-1}$, whereas the corresponding values for CdTe are 48 $kcal^{-1}$ g $atom^{-1}$ and 23.8 $kcal^{-1}$ g $atom^{-1}$, respectively.[21,22] Therefore, the CdSe binary system should be more stable over a wider temperature range than the CdTe binary system, and the highest quality $Hg_{1-x}Cd_xSe$ epilayers should be obtained at the lower end of the wider growth window, i.e. 70–90°C.

SUMMARY AND CONCLUSIONS

In this study, undoped $Hg_{1-x}Cd_xSe$ epitaxial layers of nominal thicknesses 8–14 μm have been grown by MBE on nearly lattice-matched GaSb (211)B substrates. It was found that the epilayer quality is strongly dependent on the growth temperature, as determined from x-ray diffraction, AFM, electronic transport, and minority carrier lifetime measurements. From analysis of the FWHM of XRD rocking curves, surface roughness, minority carrier lifetime, and carrier mobility, the epilayer quality was found to decrease monotonically with increasing growth temperature above 70°C. The minimum FWHM value of 116 arcsec, and the longest minority carrier lifetime of ~ 2 μs (at 77 K) were found for the lowest growth temperature, which also corresponded to epilayers with the lowest surface roughness, the most mirror-like surface, the lowest carrier concentration (low 10^{16} cm^{-3} at 130 K), and the highest electron mobility (6.6×10^4 cm^2 V^{-1} s^{-1} at 130 K).

All samples in this study were found to have an electron carrier concentration within the range 10^{16}–10^{17} cm^{-3} at 130 K, without any intentional doping, which is likely to be a major issue if these HgCdSe materials are to be useful for device fabrication. Since the background electron concentration can be reduced or increased by annealing under various conditions,[14] this suggests that as-grown $Hg_{1-x}Cd_xSe$ samples contain native defects, such as Se vacancies and/or impurities that act as n-type dopants. Despite the relatively high background electron concentration in our samples, the HgCdSe epilayers demonstrated higher mobility, longer lifetime, and lower electron concentrations in comparison to all other previous studies.[13,14,22] In future work, the source of these donor defects needs to be identified, and processes need to be developed in order to eliminate or reduce them from MBE source materials and during the growth, and/or with some form of post-growth annealing.

ACKNOWLEDGEMENTS

This work was supported by the Australian Research Council (FT130101708, DP170104562, and LE170100233), and a Research Collaboration Award from The University of Western Australia. Facilities used in this work are supported by the WA node of Australian National Fabrication Facility (ANFF).

REFERENCES

1. A. Rogalski, *Rep. Prog. Phys.* 68, 2267 (2005).
2. A. Rogalski, J. Antoszewski, and L. Faraone, *J. App. Phys.* 105, 091101 (2009).
3. W. Lei, J. Antoszewski, and L. Faraone, *Appl. Phys. Rev.* 2, 041303 (2015).
4. R.N. Jacobs, M. Jaime Vasquez, C.M. Lennon, C. NozakiL, A. Almeida, J. Pellegrino, J. Arias, C. Taylor, and B. Wissman, *J. Electron. Mater.* 44, 3076 (2015).
5. S.D. Chen, L. Lin, X.Z. He, Z.Y. Xu, C.P. Luo, and J.Z. Xu, *J. Cryst. Growth* 140, 287 (1994).
6. D.J. Smith, S.C.Y. Tsen, D. Chandrasekhar, P.A. Crozier, S. Rujirawat, G. Brill, Y.P. Chen, R. Sporken, and S. Sivananthan, *Mater. Sci. Eng.* B77, 93 (2000).
7. M. Carmody, J.G. Pasko, D. Edwall, E. Piquette, M. Kangas, S. Freeman, J. Arias, R. Jacobs, W. Mason, A. Stoltz, Y. Chen, and N.K. Dhar, *J. Electron. Mater.* 37, 9 (2008).
8. R. Gu, W. Lei, J. Antoszewski, I. Madni, G. Umana-Membreno, and L. Faraone, in *Proceedings of SPIE 9819, Infrared Technology and Applications,* XLII, 98191Z (2016).
9. W. Lei, R.J. Gu, J. Antoszewski, J. Dell, G. Neusser, M. Sieger, B. Mizaikoff, and L. Faraone, *J. Electron. Mater.* 44, 9 (2015).
10. W. Lei, R.J. Gu, J. Antoszewski, J. Dell, and L. Faraone, *J. Electron. Mater.* 43, 2788 (2014).
11. I. Madni, G. A. Umana-Membreno, W. Lei, R. Gu, J. Antoszewski, and L. Faraone, *J. Cryst. Res. Technol.* 1700167, 1 (2017).
12. C.R. Whitsett, J.G. Broerman, and C.J. Summers, *Semiconductor and Semimetals* (Cambridge: Academic Press, 1981), vol. 16, p. 53.
13. Y. Lansari, J.W. Cook, and J.F. Schetzina, *J. Electron. Mater.* 22, 8 (1993).
14. K. Doyle, C.H. Swartz, and J.H. Dinan, *J. Vac. Sci. Technol. B* 31, 3 (2013).
15. C.J. Summers and J.G. Broerman, *Phys. Rev. B* 21, 559 (1980).
16. S. Weng and M. Cocivera, *Chem. Mater.* 4, 615 (1992).
17. N. Matsumura, T. Sakamoto, and J. Saraie, *J. Cryst. Growth* 251, 602 (2003).
18. G.A. Umana-Membreno, J. Antoszewski, L. Faraone, E.P.G. Smith, G.M. Venzor, S.M. Johnson, and V. Phillips, *J. Electron. Mater.* 39, 1023 (2010).
19. J.D. Benson, L.A. Almeida, M.W. Carmody, D.D. Edwall, J.K. Markunas, R.N. Jacobs, M. Martinka, and U. Lee, *J. Electron. Mater.* 36, 949 (2007).
20. M. Carmody, D. Lee, M. Zandian, J. Phillips, and J. Arias, *J. Electron. Mater.* 32, 710 (2003).
21. P. Goldfinder and M. Jeunehomme, *Trans. Faraday Soc.* 59, 2851 (1963).
22. G. Brill, Y. Chen, and P. Wijewarnasuriya, *J. Electron. Mater.* 40, 8 (2011).